



CHORUS

This is the accepted manuscript made available via CHORUS. The article has been published as:

High-field magnetic ground state in $S=1/2$ kagome lattice antiferromagnet $\text{ZnCu}_3(\text{OH})_6\text{Cl}_2$

Tomoya Asaba, Tian-Heng Han, B. J. Lawson, F. Yu, C. Tinsman, Z. Xiang, G. Li, Young S. Lee, and Lu Li

Phys. Rev. B **90**, 064417 — Published 18 August 2014

DOI: [10.1103/PhysRevB.90.064417](https://doi.org/10.1103/PhysRevB.90.064417)

High Field Magnetic Ground State in $S = \frac{1}{2}$ Kagome Lattice Antiferromagnet $\text{ZnCu}_3(\text{OH})_6\text{Cl}_2$

T. Asaba¹, T.-H. Han^{2,3,4}, B. J. Lawson¹, F. Yu¹, C. Tinsman¹, Z. Xiang^{1,5}, G. Li¹, Y. S. Lee², and Lu Li¹

¹*Department of Physics, University of Michigan, Ann Arbor, MI 48109 USA*

²*Massachusetts Institute of Technology, Cambridge, Massachusetts 02139 USA*

³*James Franck Institute and Department of Physics, University of Chicago, Chicago, Illinois 60637, USA*

⁴*Materials Science Division, Argonne National Laboratory, Argonne, Illinois 60439, USA*

⁵*Department of Physics, University of Science and Technology of China, Hefei, Anhui, China 230026*

(Dated: August 5, 2014)

Herbertsmithite $\text{ZnCu}_3(\text{OH})_6\text{Cl}_2$ is a kagome lattice antiferromagnet with spin-1/2 and has been demonstrated to be a likely candidate of spin liquid by a number of recent experiments. The high field magnetization of the kagome lattice is complicated due to the presence of a few percent of extra Cu impurities sitting on the interlayer metallic sites. To determine the magnetic ground state of the kagome lattice, we measured the magnetization of a single crystalline $\text{ZnCu}_3(\text{OH})_6\text{Cl}_2$ using torque magnetometry down to the base temperatures 20 mK in intense magnetic field as high as 31 T. The high-field intrinsic magnetization from the kagome lattice turns out to be linear with magnetic field, and the magnetic susceptibility is independent of temperature at $20 \text{ mK} \leq T \leq 5 \text{ K}$. Moreover, below 2 K, several field-induced anomalies are observed in between 7 T and 15 T.

PACS numbers: 75.30.Cr, 75.30.Kz, 75.50.Ee

An exciting field of modern condensed matter physics is the quantum spin liquid, in which strong frustration leads to the lack of magnetic ordering and the emergence of novel physical phenomena in the ground state. The $S=1/2$ Heisenberg antiferromagnetic model on the kagome lattice is considered to be a likely place to find quantum spin liquids, which has been attractive in condensed matter physics¹⁻³. One of the best candidates of quantum spin liquid is Herbertsmithite ($\text{ZnCu}_3(\text{OH})_6\text{Cl}_2$), which consists of kagome planes of Cu^{2+} with antiferromagnetic interactions and interplane nonmagnetic Zn atoms⁴. Although the superexchange antiferromagnetic interaction is as strong as $J \sim 17 \text{ meV}$ ⁵, there is no sign of magnetic transition nor long range magnetic order down to $\sim 50 \text{ mK}$ ⁶. Also, recent results of neutron scattering measurements indicate that spin excitations form a continuum⁷, which is consistent with spin liquid states^{8,9}.

On the other hand, recent calculation results of density matrix renormalization group (DMRG) suggest that, in fact, the ground state of the kagome Heisenberg model is a gapped spin liquid¹⁰, while current experimental results are consistent with gapless or very small gapped spin liquid states. To elucidate the nature of the ground state, magnetization of single crystalline samples at base temperature bears crucial insights. However, measuring magnetization at low temperatures suffers from the Curie-Weiss contribution of impurities, which originate from a few percent of excess Cu^{2+} ions on interplane Zn sites¹¹. From Knight shift measurement on the Herbertsmithite samples¹², intrinsic contribution is considered to be much smaller than contribution from impurity at very low temperature. While recently g-factor anisotropy and magnetocaloric anisotropy are measured using a high quality single crystal¹³, separation of contribution from

impurity and from kagome remains a challenging task. In this letter, we applied torque magnetometry to the magnetic ground state in intense magnetic field, in which the impurity contribution should saturate. A number of field driven anomalies were observed at magnetic field $\sim 7-15 \text{ T}$, which may originate from intrinsic kagome spins. Furthermore, the magnetic susceptibility at higher field is found to be independent of field as well as temperature.

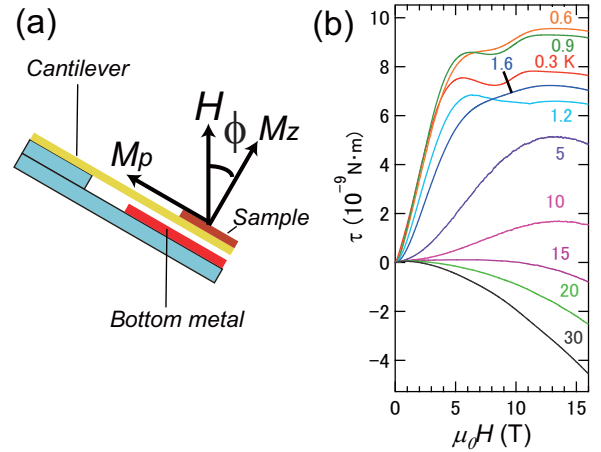


FIG. 1. (color online) (a) Sketch of cantilever setup of torque measurement. A sample is mounted to the tip of a metallic cantilever. The tilt angle is defined by the angle between the field \vec{H} and the kagome lattice normal axis (z-axis). The torque τ generated by the sample $\vec{m} \times \vec{B}$ is along the axis coming-out-of sketch page, and the torque deflects the cantilever so that the capacitance changes between the metallic cantilever and the gold film underneath. (b) The torque responses from herbertsmithite Sample A in selected T between 0.3 K and 30 K. The tilt angle $\phi = 20^\circ$.

We used torque magnetometry to measure magnetization anisotropy of the sample¹⁴. Tilt angle ϕ is the angle between the c -axis of herbertsmithite (the normal axis of the kagome plane) and the magnetic field (Fig. 1(a)). Torque is described as follows,

$$\vec{\tau} = \mu_0 V \vec{M} \times \vec{H} \quad (1)$$

And the amplitude of torque τ is found¹⁵ to be

$$\tau = M_p \mu_0 H_z V - M_z \mu_0 H_p V \quad (2)$$

where V is the sample volume, M_p is the magnetization in plane, M_z is the magnetization along the crystalline c -axis, H_z is the magnetic field projected along the c -axis, and H_p is the magnetic field projected in the kagome plane. We note that in the low-field limit magnetization is proportional to the susceptibility, as $M_p = \chi_p H_p$ and $M_z = \chi_z H_z$. Therefore, in the low-field limit, Eq. 2 leads to $\tau \sim \mu_0 \Delta\chi H^2 V \sin\phi \cos\phi$, where the susceptibility anisotropy $\Delta\chi = \chi_p - \chi_z$ is the difference between the c -axis susceptibility χ_z and the in plane susceptibility χ_p .

$\text{ZnCu}_3(\text{OH})_6\text{Cl}_2$ was grown with powder samples that were first synthesized inside a sealed quartz tubing and transported under a temperature gradient in a three-zone furnace for crystallization¹⁶. We measured two samples, Sample A (volume $\sim 0.3 \text{ mm} \times 0.3 \text{ mm} \times 0.4 \text{ mm}$) and B (volume $\sim 0.1 \text{ mm} \times 0.1 \text{ mm} \times 0.2 \text{ mm}$). Based on X-ray anomalous dispersion spectroscopy¹¹, there are 15% interlayered Cu in Sample A, and 25% interlayered Cu in Sample B. None of the samples show signature of Zn mixing into the Cu kagome plane. This is in contrast to the case in powder samples in which NMR studies found that there was Zn mixing into the Cu kagome plane¹⁷. Each sample was mounted on thin cantilevers with c -axis facing-up and the magnetic torque was measured capacitively, as shown in Fig. 1(a).

Example curves of the field dependence of the magnetic torque τ are shown in Fig. 1(b), measured on Sample A at selected temperatures T between 0.3 K and 30 K. The tilt angle ϕ is 20 degrees. In Fig. 1(b), the positive sign of τ is consistent with the sign in Eq. 2, which means that the torque component from the c -axis magnetization $M_z H_p$ is smaller than that from the in-plane magnetization $M_p H_z$. As shown in Fig. 1(b), the torque response becomes quadratic at higher T and torque changes sign around $T \sim 15 \text{ K}$. Those facts are consistent with previous measurements^{13,18} in which the c -axis susceptibility χ_z was shown to be slightly larger than the in-plane susceptibility χ_p at $T \geq 15 \text{ K}$.

At low T , the $\tau - H$ curve shows two sets of interesting features: (1) $\tau - H$ is non-monotonic; (2) at $\mu_0 H \sim 8 \text{ T}$, a number of kinks are observed in the $\tau - H$ curves. We focus on the kinks that suggest magnetic-field-driven anomalies, then analyze the magnetization curves in intense magnetic fields. The high field magnetic susceptibility is found to be H -independent and T -independent (Pauli-like) in the $S = \frac{1}{2}$ kagome system below 5 K.

The field-driven anomalies are emphasized by taking derivatives of torque τ with respect to field H . Fig. 2(a)

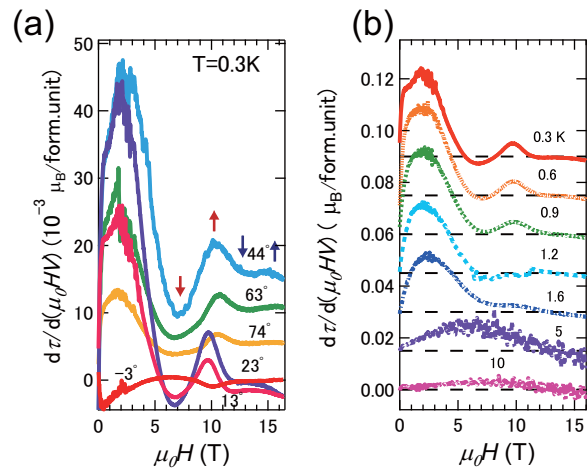


FIG. 2. (color online) (a) The derivative $\frac{d\tau}{dH}$ vs. field H of Herbertsmithite Sample A at selected tilt angles ϕ . The signal is normalized to crystal formula unit. (b) Temperature dependence of the derivative $\frac{d\tau}{dH}$, at $\phi \sim 20^\circ$. For clarity, the curves are vertically displaced and the origin of each curve is marked by the dashed lines near zero H . The anomaly fields show almost no dependence of tilt angle and temperature.

shows the angular dependence of derivative $\frac{d\tau}{dH}$ from $\phi = -3$ degrees to 74 degrees at 0.3 K . In high magnetic fields, we have observed four possible field-induced anomalies. They are marked by two pairs of arrows, at $\mu_0 H \sim 7 \text{ T}$ and 10 T , and $\mu_0 H \sim 13 \text{ T}$ and 15 T . The first pair is so pronounced that there are clear slope changes in the $\tau - H$ curves in Fig. 1(b).

The anomaly fields are almost independent of the magnetic field orientation, which is consistent with Heisenberg model. As the field tilt angle changes from -3° to 74° , the peaks and dips shift as little as 1 T , compared with the anomaly field values on the order of $\sim 10 \text{ T}$. Moreover, measurements at different T show that the anomaly fields are almost T independent. Fig. 2(b) shows the $\frac{d\tau}{dH}$ vs. $\mu_0 H$ at selected T between 0.3 K and 10 K . The field locations for these anomalies do not show noticeable changes for $T < 1 \text{ K}$. The pair of higher field features (13 T and 15 T) disappear at $T > 1.2 \text{ K}$, while the pair of lower field features disappears at $T > 1.6 \text{ K}$. Below 2 K , all the anomaly field values are almost T independent. For Sample B, we further cool down to 20 mK . The derivative $\frac{d\tau}{dH}$ is almost independent of T between 20 mK and 330 mK .

The trend of low T torque signal is consistent with earlier magnetization measurements¹³. We find that the increase of the magnetization contribution from impurity would make the torque signal more positive, whereas the increase of the kagome plane magnetization would make the torque signal more negative. In the earlier magnetization measurements¹³ at $1.8 \text{ K} \leq T \leq 300 \text{ K}$, $(\chi_z/\chi_p)_{\text{imp}} < 1$ and $(\chi_z/\chi_p)_{\text{kagome}} > 1$.

To further understand the competition between M_z and M_p , we look at the effective transverse magnetization

M_T , which is defined as

$$M_T = \frac{\tau}{\mu_0 HV} \quad (3)$$

The resulting M_T curves are shown in Fig. 3(a). Above 1 K at zero field the slope of the M_T vs. H curves increases greatly as T decreases, following the Curie-Weiss law, which is consistent with early results^{12,19}. At higher fields, the slope becomes negative, because the intrinsic kagome moments prefer stay along the crystalline c -axis, i.e., have larger contribution from M_z . Furthermore, the fact that the slope above 10 T does not change when T increases suggests that the intrinsic magnetic susceptibility from the kagome lattice is T independent below 5 K.

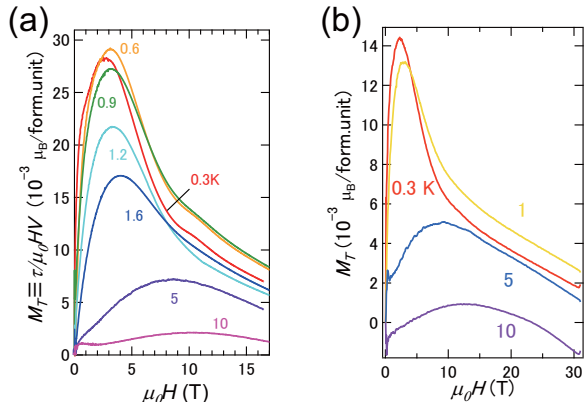


FIG. 3. (color online) (a) The effective transverse magnetization M_T vs. magnetic field H of Sample A at H up to 18 T at $\phi = 20^\circ$. M_T is defined as $\tau/\mu_0 HV$. (b) The M_T vs. H curve of Sample B at H up to 31 T at $T = 0.3$ K and $\phi \sim 65^\circ$.

To further illustrate this point, the effective magnetic susceptibility is defined as $\chi_{eff} \equiv \frac{1}{\mu_0} \frac{dM_T}{dH}$. Fig. 4(a) displays χ_{eff} vs. field H using the 31 T data shown in Fig. 3(b). At $H \geq 15$ T, χ_{eff} stays constant at $T \leq 5$ K. We have measured the high field χ_{eff} in the Sample B in two temperature ranges, first above 300 mK using a Helium-3 refrigerator, and then down to 20 mK taken in a dilution-refrigerator Fig. 4(b) displays the T dependence of the absolute value of the high-field susceptibility χ_{eff} , which is the slope of the M_T vs. H curves at $H \geq 15$ T. As shown in Fig. 4(b), the high field magnetic susceptibility is almost independent of T below 5 K. This is consistent with the presence of a spinon Fermi surface as is also observed in triangular organic antiferromagnetic systems²³.

We note that the effective magnetic susceptibility detects only the anisotropic part of the magnetic susceptibility. Assuming the anisotropy stays the same for the kagome lattice at different H , we infer that the magnetic susceptibility itself is T -independent and H -independent in the intense fields. In triangular organic antiferromagnetic systems²³, torque measurement

has demonstrated that the intrinsic magnetic susceptibility is proportional to the effective magnetic susceptibility.

Figure 4(c) summarizes the phase diagram of herbertsmithite. At $\mu_0 H < 7$ T, the magnetic signal of herbertsmithite consists of the kagome plane signal M_z and the impurity contributions M_{imp} from the interlayered Cu magnetic moments. The impurity contribution quickly saturates as H increases. As H increases to 7 T, the magnetizations of all the impurities become constant. At 8 T $< H < 16$ T, we observe that two pairs of field-induced anomalies are independent of T at $20 \text{ mK} \leq T \leq 1.6$ K.

Discussion For Cu spins with g -factor of 2, 10 T magnetic field corresponds to $\sim 0.07J$, where J is the exchange energy of this material. It is worth emphasizing that the strong applied field introduces a Zeeman energy of $\sim 0.1J$. This complicates a direct comparison with theories considering only a Heisenberg term¹⁰. A recent high-field specific heat study on a single crystal herbertsmithite indicates a strong field-dependence below 9 T which significantly weakens from 9 T to 18 T²⁴. This corroborates with our torque measurements, both of which are consistent with herbertsmithite entering a high-field regime at $\mu_0 H > 10$ T.

Our field-induced anomalies extend from 20 mK to 1.6 K and stay at certain field magnitudes. This is distinct from those observations in NMR on powder samples²⁰, which have field dependent transition temperature that stay below 0.6 K up to 12 T. The origin of the anomalies is still an open question. These anomalies can arise from the interlayered Cu magnetic moments, potentially through coupling with the kagome planes. The caveat of this simple explanation is that the anomaly fields are not correlated with the concentration level of the interlayered Cu.

At low T , the T -independent kagome-intrinsic susceptibility is consistent with a spinon Fermi surface state at high fields. Similar behaviors have been observed on an organic spin liquid featuring a triangular spin lattice²³. The existence of a spinon Fermi surface at high fields is also supported by the large gamma term of specific heat in high fields²⁴, as well as the early ¹⁷O NMR studies²⁵. Latest theories predict magnetic ordering at higher field²⁷, including a field-induced spontaneous breaking of spin rotational symmetry on a kagome gapless Dirac spin liquid²⁸. The transition temperature and ordered moment both scale with the applied field, at odds with our torque data and the high-field specific heat measurements²⁴. For a kagome spin lattice, a magnetization plateau may exist at $1/9$ of the saturation²⁶, which corresponds to $\mu_0 H \sim 50 \text{ T}$ ²⁴, much higher than our anomaly fields. We further note that the anomaly fields stay almost the same as \vec{H} changes from along the c -axis to the ab -plane, suggesting the Heisenberg symmetry is behind these anomalies.

Although being dominated by an isotropic Heisenberg exchange, the actual spin Hamiltonian of herbertsmithite is complicated by perturbations. The leading terms are likely the Dzyaloshinskii-Moriya (DM) interaction^{18,21,22},

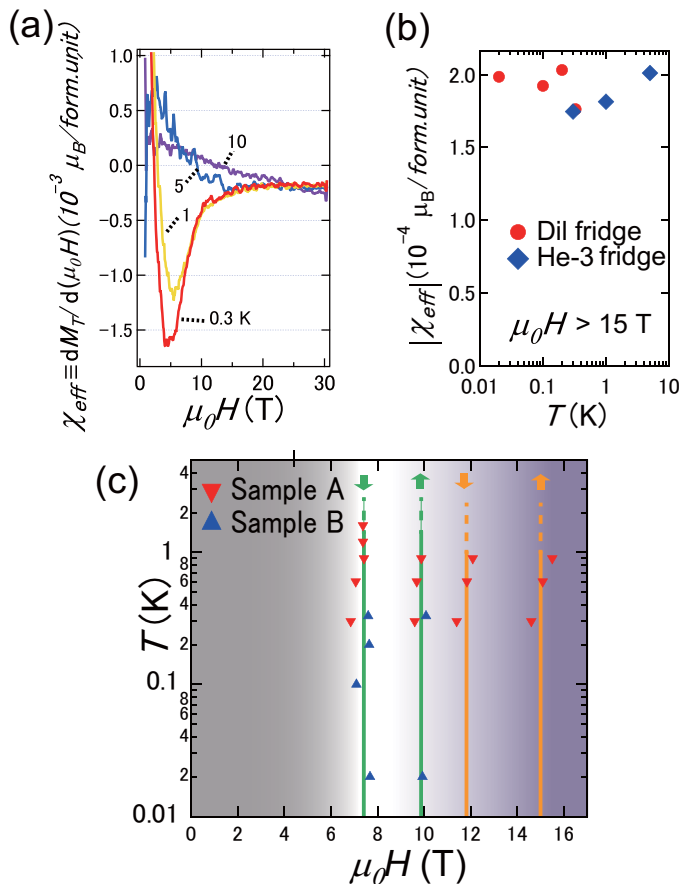


FIG. 4. (color online) (a) The effective magnetic susceptibility $\chi_{eff} \equiv \frac{dM_T}{\mu_0 dH}$ is plotted as function of field H up to 31 T for Sample B. For curves at $T \leq 5$ K, χ_{eff} is found to be constant at fields above 15 T. (b) The temperature T dependence of the absolute value of the high field χ_{eff} of the kagome lattices. The red solid circles are from the torque measurements performed in a dilution refrigerator (marked as dil-fridge) up to 18 T. The blue squares are the effective magnetic susceptibility data in a Helium-3 refrigerator (marked as He-3 fridge) as in Panel a. (c) The $T-H$ phase diagram of herbertsmithite obtained from torque measurement. Two pairs of solid lines are eye guides drawn for the field-driven anomalies. Arrows indicate whether the field corresponds to the minimum (down) or maximum (up) in the $d\tau/dH$ curve. In the low field shaded area, the magnetic torque from both impurity and the intrinsic contributions are mixed. In the field range 7 T - 10 T, the impurity contribution is fully saturated. At H above 10 T, the magnetization change arises mainly from the kagome plane.

easy-axis anisotropic exchange energy¹³ and coupling energy to the impurities¹¹, whose magnitudes are consistent with the 10% variation of the anomalous field values when rotating the crystal in field. Other perturbations are present but may be smaller, such as kagome-kagome direct coupling and second-nearest-neighbor interaction

in plane²⁹. In the $T \rightarrow 0$ K limit, the DM interaction, for various combinations of in-plane and normal-to-plane components, causes an increasing easy-axis magnetization anisotropy^{30,31}. The quantitative determination of this is hampered at $T < 30$ K by the spin-cluster size. Differently, the effect of an exchange anisotropy on magnetization anisotropy shows a vanishing tendency as $T \rightarrow 0$ K. The combined effect of easy-axis kagome-intrinsic magnetization anisotropy due to the DM term and the easy-plane magnetization anisotropy of the impurities, both of which are on the order of 10%, might explain the weak sample magnetization anisotropy at low T .

The anomaly fields are comparable to the energy scale of major perturbations. The closeness in energy may have produced those two pairs of anomalies and opened up new possibilities to explain the nature of the observed crossovers. Additional theories which include at least one of the major perturbations on a large lattice cluster are strongly desired. Further, torque magnetometry is only sensitive to magnetization anisotropy. A better understanding of our torque data requires a precise determination of uniform susceptibility in the same temperature and dc field ranges. When quantum fluctuations and geometric frustration prohibit the system from long-range spin ordering, the dynamic spin correlations at low frequencies contain essential clues which provide supplementary information to thermodynamic studies. This calls for further neutron scattering experiments at low energies and high fields. Both works are currently in progress.

Conclusion We studied the high field magnetic torque of kagome lattice single crystalline $\text{ZnCu}_3(\text{OH})_6\text{Cl}_2$ and observed field-induced anomalies. The field-induced anomalies that are observed between 7 T and 15 T hint at subtle changes to the correlations of the moments of interlayered Cu. The effective magnetic susceptibility is almost independent of temperature at $20 \text{ mK} \leq T \leq 5 \text{ K}$ at intense magnetic fields, indicating a gapless spin liquid state.

Acknowledgement This work at the University of Michigan is supported by the U.S. Department of Energy, Office of Basic Energy Sciences, Division of Materials Sciences and Engineering under Award DE-SC0008110. The work at MIT is supported by the U.S. Department of Energy under Grant No. DE-FG02-07ER46134. T. Asaba thanks the support from the Nakajima Foundation. T.-H. Han acknowledges the support by the Grainger Fellowship from the Department of Physics, University of Chicago during data analysis and manuscript writing. B. J. L. thanks the support from the National Science Foundation Graduate Fellowship grant No. F031543. We are grateful for the discussions with P.A. Lee, S. Sachdev and Kai Sun. The high-field experiments were performed at the National High Magnetic Field Laboratory, which is supported by NSF Cooperative Agreement No. DMR-084173, by the State of Florida, and by the DOE.

-
- ¹ P.W. Anderson, *Mater. Res. Bull.* **8**, 153 (1973).
 - ² P.W. Anderson, *Science* **235**, 1196 (1987).
 - ³ L. Balents, *Nature* **464**, 199 (2010).
 - ⁴ M. P. Shores, E. A. Nytko, B. M. Bartlett, and D. G. Nocera, *J. Am. Chem. Soc.* **127**, 13462 (2005).
 - ⁵ J. S. Helton, K. Matan, M. P. Shores, E. A. Nytko, B. M. Bartlett, Y. Yoshida, Y. Takano, A. Suslov, Y. Qiu, J.-H. Chung, D. G. Nocera, and Y. S. Lee, *Phys. Rev. Lett.* **98**, 107204 (2007).
 - ⁶ P. Mendels, F. Bert, M. A. de Vries, A. Olariu, A. Harrison, F. Duc, J. C. Trombe, J. S. Lord, A. Amato, and C. Baines, *Phys. Rev. Lett.* **98**, 077204 (2007).
 - ⁷ T.-H. Han, J. S. Helton, S. Chu, D. G. Nocera, J. A. Rodriguez-Rivera, C. Broholm, and Y. S. Lee, *Nature* **492**, 406 (2012).
 - ⁸ Dirk Wulferding, Peter Lemmens, Patric Scheib, Jens Roder, Philippe Mendels, Shaoyan Chu, Tianheng Han, and Young S. Lee, *Phys. Rev. B* **82**, 144412 (2010).
 - ⁹ M. A. de Vries, K. V. Kamenev, W. A. Kockelmann, J. Sanchez-Benitez, and A. Harrison, *Phys. Rev. Lett.* **100**, 157205 (2008).
 - ¹⁰ S. Yan, D. Huse, and S. White, *Science* **332**, 1173 (2011).
 - ¹¹ Danna E. Freedman, Tianheng H. Han, Andrea Prodi, Peter Muller, Qing-Zhen Huang, Yu-Sheng Chen, Samuel M. Webb, Young S. Lee, Tyrel M. McQueen, and Daniel G. Nocera, *J. Am. Chem. Soc.* **132**, 16185 (2010).
 - ¹² T. Imai, M. Fu, T. H. Han, and Y. S. Lee, *Phys. Rev. B* **84**, 020411R (2011).
 - ¹³ T. Han, S. Chu and Y. S. Lee, *Phys. Rev. Lett.* **108**, 157202 (2012).
 - ¹⁴ L. Li, C. Richter, J. Mannhart, and R. C. Ashoori, *Nature Phys.* **7**, 762 (2011).
 - ¹⁵ Lu Li, J. G. Checkelsky, Y. S. Hor, C. Uher, A. F. Hebard, R. J. Cava, N. P. Ong, *Science* **321**, 547 (2008).
 - ¹⁶ T. H. Han, J. S. Helton, S. Chu, A. Prodi, D. K. Singh, C. Mazzoli, P. Muller, D. G. Nocera, and Y. S. Lee, *Phys. Rev. B* **83**, 100402R (2011).
 - ¹⁷ A. Olariu, P. Mendels, F. Bert, F. Duc, J. C. Trombe, M. A. de Vries, and A. Harrison, *Phys. Rev. Lett.* **100**, 087202 (2008).
 - ¹⁸ A. Zorko, S. Nellutla, J. van Tol, L. C. Brunel, F. Bert, F. Duc, J.-C. Trombe, M. A. de Vries, A. Harrison, and P. Mendels, *Phys. Rev. Lett.* **101**, 026405 (2008).
 - ¹⁹ F. Bert, S. Nakamae, F. Ladieu, D. LHote, P. Bonville, F. Duc, J.-C. Trombe, and P. Mendels, *Phys. Rev. B* **76**, 132411 (2007).
 - ²⁰ M. Jeong, F. Bert, P. Mendels, F. Duc, J. C. Trombe, M. A. de Vries, and A. Harrison, *Phys. Rev. Lett.* **107**, 237201 (2011).
 - ²¹ Daniel Grohol, Kittiwit Matan, Jin-Hyung Cho, Seung-Hun Lee, Jeffrey W. Lynn, Daniel G. Nocera, and Young S. Lee, *Nature Mater.* **4**, 323 (2005).
 - ²² M. Elhajal, B. Canals, and C. Lacroix, *Phys. Rev. B* **66**, 014422 (2002).
 - ²³ D. Watanabe, M. Yamashita, S. Tonegawa, Y. Oshima, H.M. Yamamoto, R. Kato, I. Sheikin, K. Behnia, T. Terashima, S. Uji, T. Shibauchi, and Y. Matsuda, *Nature Commun.* **3**, 1090 (2012).
 - ²⁴ Tian-Heng Han, Robin Chisnell, Craig J. Bonnoit, Danna E. Freedman, Vivien S. Zapf, Neil Harrison, Daniel G. Nocera, Yasu Takano, and Young S. Lee, arXiv:1402.2693 (2014).
 - ²⁵ P. Mendels, and F. Bert, *J. Phys. Soc. Jpn.* **79**, 011001 (2010).
 - ²⁶ S. Nishimoto, N. Shibata, and C. Hotta, *Nat. Commun.* **4**, 2287 (2013).
 - ²⁷ Z.Hao and O. Tchernyshyov, *Phys. Rev. B* **87**, 214404 (2013).
 - ²⁸ Y. Ran, W.-H. Ko, P.A. Lee, and X.-G. Wen, *Phys. Rev. Lett.* **102**, 047205 (2009).
 - ²⁹ H. O. Jeschke, F. Salvat-Pujol, and R. Valenti, *Phys. Rev. B*, **88**, 075106 (2013).
 - ³⁰ M. Rigol and R. R. P. Singh, *Phys. Rev. Lett.*, **98**, 207204 (2007).
 - ³¹ M. Rigol and R. R. P. Singh, *Phys. Rev. B*, **76**, 184403 (2007).